

Development of Three-Dimensional Deformable Flexible Printed Circuit Boards Using Ag Flake-Based Conductors and Thermoplastic Polyamide Substrates

Aram Lee¹, Minji Kang², Do Young Kim³, Hee Yoon Jang³, Ji-Won Park⁴,
Tae-Wook Kim^{5,6}, Jae-Min Hong⁷ , and Seung-Ki Lee³ 

¹ Electronics and Telecommunications Research Institute, Honam Research Division, AI Convergence Research Section, Gwangju 61012, Korea

² Chemical Materials Solutions Center, Korea Research Institute of Chemical Technology, Daejeon 34114, Korea

³ School of Materials Science and Engineering, Pusan National University, Busan 46241, Korea

⁴ R & D Center of JB Lab Corporation, Seoul 08788, Korea

⁵ Department of Flexible and Printable Electronics, Jeonbuk National University, Jeonju 54896, Korea

⁶ Department of JBNU, KIST Industry-Academia Convergence Research, Jeonbuk National University, Jeonju 54896, Korea

⁷ Soft Hybrid Materials Research Center, Korea Institute of Science and Technology, Seoul 02792, Korea

(Received April 14, 2024; Revised April 18, 2024; Accepted April 19, 2024)

Abstract: This study proposes an innovative methodology for developing flexible printed circuit boards (FPCBs) capable of conforming to three-dimensional shapes, meeting the increasing demand for electronic circuits in diverse and complex product designs. By integrating a traditional flat plate-based fabrication process with a subsequent three-dimensional thermal deformation technique, we have successfully demonstrated an FPCB that maintains stable electrical characteristics despite significant shape deformations. Using a modified polyimide substrate along with Ag flake-based conductive ink, we identified optimized process variables that enable substrate thermal deformation at lower temperatures (~130°C) and enhance the stretchability of the conductive ink ($\epsilon \sim 30\%$). The application of this novel FPCB in a prototype 3D-shaped sensor device, incorporating photosensors and temperature sensors, illustrates its potential for creating multifunctional, shape-adaptable electronic devices. The sensor can detect external light sources and measure ambient temperature, demonstrating stable operation even after transitioning from a planar to a three-dimensional configuration. This research lays the foundation for next-generation FPCBs that can be seamlessly integrated into various products, ushering in a new era of electronic device design and functionality.

Keywords: Flexible printed circuit boards, 3D shape deformation, Flake based Ag ink, Thermal deformation processing, Stretchable electronics

1. INTRODUCTION

The rapid development of mobile electronics and advancements in products integral to daily life, such as transformable displays and automobiles, have spurred a demand for electronic circuit systems that conform to the diverse shapes of these products [1-3]. Particularly for the development of electronic systems with groundbreaking

✉ Jae-Min Hong; jmhong@kist.re.kr

Seung-Ki Lee; ifriend@pusan.ac.kr

Aram Lee and Minji Kang equally contributed to this work.

Copyright ©2024 KIEEME. All rights reserved.

This is an Open-Access article distributed under the terms of the Creative Commons Attribution Non-Commercial License (<http://creativecommons.org/licenses/by-nc/3.0>) which permits unrestricted non-commercial use, distribution, and reproduction in any medium, provided the original work is properly cited.

functionality, advanced circuit boards are critically needed to accommodate various product shapes [4,5]. To date, research has predominantly focused on stretchable electrode materials and flexible substrates designed for three-dimensional shapes [6-8]. However, the advancement of printed circuit board (PCB) processing technology, which integrates electrodes and substrates, has not progressed impressively. Flexible printed circuit boards (FPCBs) represent a category of PCBs characterized by their conductive wiring that links each component within electronic device constructions [9]. These boards are designed for flexibility, utilizing a polymer substrate and having a thin, bendable, and lightweight nature. This allows for an efficient layout of circuit boards within the constrained spaces of electronic devices, offering the benefits of streamlined design for compact precision electronic devices and enhanced design flexibility. Commercialized FPCBs are constructed from dynamic laminated plates, featuring a thin layer of metal line on both the top and bottom surfaces of polyimide material. They can be categorized into single-sided, double-sided, multi-layer, and rigid-flex circuits based on the number of functional layers [10-12]. Nevertheless, existing FPCBs, being film-type products, are constrained by the bendability of their polyimide-based materials, limiting their formability and stretchability [13,14]. Therefore, to meet the diversification needs of next-generation displays and wearable electronics, it is imperative to develop materials and manufacturing processes for next-generation FPCBs that can be custom-molded into varied shapes, including three-dimensional forms.

In this study, we propose a method to create three-dimensional shape deformable FPCBs through post-processing after manufacturing electronic devices. This approach utilizes the conventional flat plate-based process, subsequently transforming them into desired three-dimensional shapes using the thermal deformation method. By modifying the physical properties of a polyimide substrate, we enabled its heat deformation processing at relatively low temperatures (approximately 130°C) and incorporated silver flakes-based conducting ink to enhance stretchability. Additionally, we identified the correlation between the curing speeds of the conductive ink and substrate during 3D thermal deformation, from which optimized process variables were derived. This led to the development of an FPCB capable of maintaining stable electrical characteristics despite shape

deformations of up to 30%. Applying this FPCB, we demonstrated a prototype three-dimensional sensor combining a temperature sensor and an optical sensor. This sensor retained stable sensing functionality after transitioning from a flat to a three-dimensional pyramid structure, capable of simultaneously detecting the direction of an external light source and measuring the surrounding temperature. The development of these shape-customizable FPCB boards holds significant potential for overcoming existing limitations and adapting to various products.

2. EXPERIMENTAL DETAILS

2.1 Strain-stress analysis at different temperatures

To evaluate the mechanical properties of polyimide (PI) films, we meticulously analyzed their stress-strain curves at 25°C and 130°C. Dog bone-shaped specimens were crafted from the PI films in a standardized shape to ensure uniform stress distribution during testing. These specimens underwent tensile tests within a temperature-controlled chamber attached to a universal testing machine, enabling precise control over the testing environment.

2.2 TGA analysis

The thermal decomposition temperature was determined using thermogravimetric analysis (TGA) on a TGA4000 instrument (PerkinElmer). The analysis covered a temperature range from 30 to 800°C, with a heating rate of 10°C per minute under a nitrogen atmosphere.

2.3 3D deformation of Ag ink/PI based FPCB

To efficiently shape Ag ink/PI-based FPCBs into three-dimensional forms following the flat-plate fabrication process, both a convection oven and a specially designed mold are necessary. In this study, we employed a pyramid-shaped mold with its apex removed; however, cylindrical and dome-shaped molds are also viable options. Once the oven reaches the optimal temperature of 130°C, the Ag ink/PI-based FPCB is

securely affixed to the mold and placed inside for thermal deformation processing. The speed of this transformation can be controlled by applying a weight to the end of the FPCB, utilizing gravitational force to apply pressure. After a 2-minute thermal deformation process, the FPCB and mold are removed together and allowed to stand for 5 minutes before being gradually cooled using air circulation. Once adequately cooled, the FPCB is carefully detached from the mold.

3. RESULTS AND DISCUSSION

Figure 1(a) illustrates a schematic representation of the manufacturing process used to fabricate a functional electronic device, starting from a planar approach and transitioning into a three-dimensional setup. The process involves the use of Ag nanoflake-based conductive ink (QVO-Ink_R, ITIZ), known for its impressive elasticity. This ink is printed onto a modified polyimide (PI) substrate, which has been treated to achieve specific physical properties using conventional printed circuit techniques. To synthesize modified polyimide films with desired thermal and mechanical properties, C36-diamine, ODA (oxydianiline), and NMP (N-Methyl-2-pyrrolidone)

were weighed and mixed in the ratio of 10.6:1:37.5 in a polymer synthesis reactor under a nitrogen atmosphere for 1 hour to ensure a uniform blend. The mechanical flexibility and toughness of the modified polyimide film can be adjusted by controlling the amount of ODA, which contains ether linkages. Subsequently, a BPADA slurry was slowly introduced into the mixture and continuously stirred for 7 hours to facilitate controlled polymerization. BPADA acts as a critical agent in this context by promoting the formation of imide rings, which are essential for achieving desired levels of thermal stability and mechanical strength. This is due to BPADA's unique aromatic backbone, which enhances the polymer matrix's cross-linking capabilities [15]. The ink deposited on this substrate contains flake-type fillers capable of maintaining stable electrical resistance values even under mechanical stretching, due to the planar contact between individual flakes. The minimum linewidth of the printed Ag electrode is approximately 100 μm , with the thickness adjustable through repeated printing. Following this step, solder paste is applied at the contact points to facilitate the mounting of optical diodes, concluding the planar phase of device fabrication. Subsequently, the device undergoes a thermal deformation process using a pre-fabricated mold

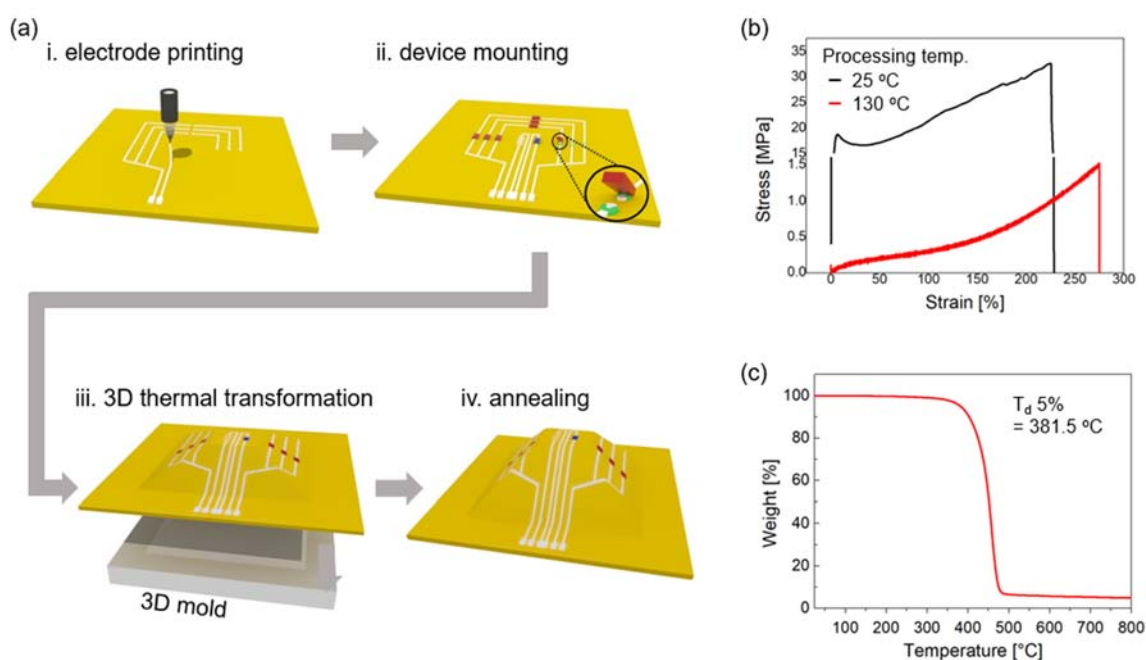


Fig. 1. (a) Schematic illustration of the fabrication process and 3D deformation of the FPCB, (b) strain-stress curve at various analysis temperatures and (c) thermogravimetric analysis (TGA) thermograms of the Ag flake ink/PI-based FPCB.

designed to give it a three-dimensional shape, carried out at a temperature of 130°C. During this thermal process, the mechanical properties of the PI substrate change to enhance malleability, facilitating the molding process [as shown in Fig. 1(b)]. A critical factor in this process is the duration of thermal treatment. It's important to determine the appropriate duration for adequate thermal treatment to ensure that the Ag conducting ink does not fully cure, even if the substrate undergoes sufficient transformation. Insufficient thermal treatment time may cause uneven stress on the substrate, potentially leading to tearing. Conversely, excessive duration may prematurely harden the Ag ink, resulting in short-circuiting issues. The parameters optimized for the thermal deformation process, aimed at achieving the desired three-dimensional configuration, are set at 130°C for 2 minutes. It's important to note, however, that these conditions may vary depending on the target deformation structure and ink deposition parameters. The transformation process concludes with a final thermal treatment at 150°C for 5 minutes to fully cure the Ag ink, ensuring the chemical stability of the substrate up to 400°C, as shown by the Thermogravimetric Analysis (TGA) results in Fig. 1(c).

To assess the maximum stretchability achievable by 2D flake-based Ag electrodes on the stretchable PI substrate, we quantitatively analyzed their mechanical-electrical properties relationship under conditions of 3D thermal deformation. After printing Ag electrodes with a line width of 150 μm on the PI substrate, we subjected them to uniaxial tensile strain

for 2 minutes at a temperature of 130°C, followed by an analysis of electrical conductivity. Figure 2(a) depicts the sample with an electrode pattern array, featuring a channel length of 3 cm, printed over a 5 cm × 5 cm area. At this time, the Ag flakes that make up the printed ink have a size of 1 to 3 μm [Fig. 2(a) inset]. Subsequently, longitudinal tension was applied using homemade stretching equipment. Figure 2(b) shows an Optical Microscopy (OM) image capturing the morphological changes within the channel area stretched by increments of 10%, ranging from 10% to 50% compared to its original length. It was observed that the channel width progressively decreased with increasing stretching rates. Notably, at a stretching rate of 40%, the electrode fractured at its most vulnerable point within the channel. At a stretch of 50%, the electrode experienced complete rupture, exposing the underlying PI substrate. The results of the electrical conductivity evaluation, conducted alongside the OM analysis, are presented simultaneously in Fig. 2(c). Statistical analysis concluded that the Ag electrode can maintain stable electrical properties within a range of 2.2 S to 2.7 S, up to a tensile strain of 30%. This impressive elasticity is primarily attributed to the 2D flake composition of the Ag conductive ink, which enables sustained broad contact across a wide area even during stretching deformations [16,17]. Additionally, the thermal treatment duration of 2 minutes proved insufficient for complete solvent volatilization within the Ag ink, allowing the Ag flakes to undergo adequate displacement. However, once the deformation exceeded 30%, a noticeable decrease in

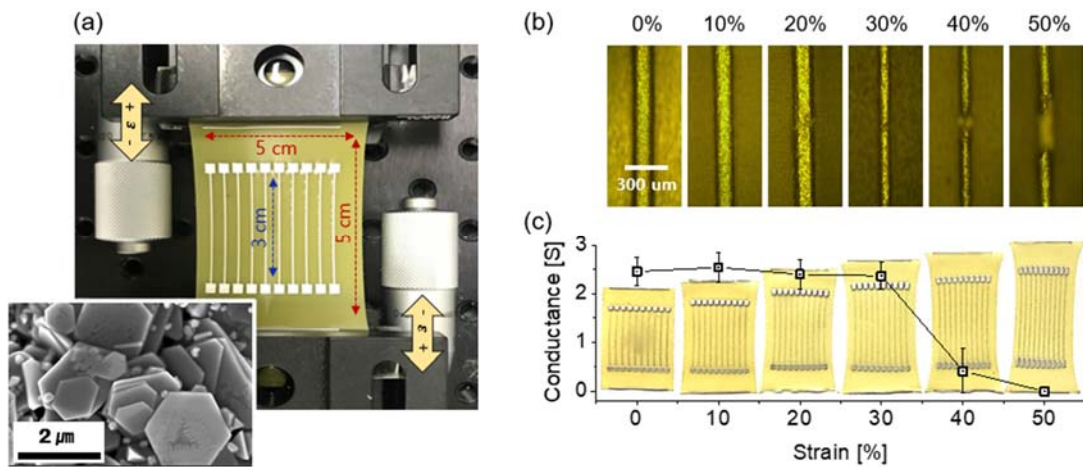


Fig. 2. (a) Micro-control of longitudinal strain application and SEM image of Ag flakes (inset), (b) optical microscope images of line-patterned electrodes under varying strains, and (c) electrical conductivity of electrodes at different strain levels.

conductivity occurred due to the inability to sustain inter-flake contact. Beyond a deformation rate of 50%, the electrode experienced a complete short circuit, leading to total loss of conductivity. Hence, it's crucial to establish a correlation between the ink's dimension, thickness, and the elongation rate to define an optimal thermal treatment time parameter suited to the specific structural requirements of the intended circuit.

Subsequent analyses aimed to assess the stability and durability of the shape-transformable Ag electrode and substrate configurations under deformation induced by external stress. This assessment involved monitoring the temporal behavior of electrical properties. For this purpose, a test sample was fabricated, integrating a photodiode onto an electrode/substrate assembly strained by 20% and 30% as experimental groups. The chosen deformation range corresponds to the section that exhibited stable operation in the electrical-mechanical deformation analysis results previously depicted in Fig. 2. Additionally, a control sample, without any applied stress, was prepared for comparative analysis. Upon applying bias to this test sample, the photodiode activated to emit light, enabling observation of visual changes and simultaneous monitoring of the resistance change rate (R/R_0), as depicted in Figs. 3(a)~(c). Initially, to establish control data, the temporal characteristics of resistance change were monitored under

ambient conditions (average temperature = 29°C, humidity = 47%). This analysis revealed that both the tensioned sample and the control sample maintained stable electrical characteristics for approximately 96 hours, as shown in Fig. 3(b). This observation suggests that applying up to 30% tension does not adversely affect the stability of the substrate, electrode, diode, or the interconnectivity between the electrode and diode.

Moreover, the lifespan and reliability of the test sample under extreme operating conditions were evaluated by exposing it to stress conditions marked by 85% humidity and a temperature of 85°C. The results, summarized in Fig. 3(c), revealed some instability in the resistance change rate due to the elevated humidity levels. However, it was concluded that the electrical characteristics of the test sample remained intact with no notable degradation, emphasizing its robustness and reliability even in adverse conditions.

To demonstrate the viability of the proposed methodology, which involves three-dimensionalization following a flat plate-based fabrication process, we fabricated and evaluated a prototype multi-sensor device oriented in three dimensions. Figure 4(a) illustrates the planar circuit diagram of an integrated sensor element, comprising a photodiode for detecting external light, a resistance temperature detector (RTD) for sensing temperature variations, and an electrode

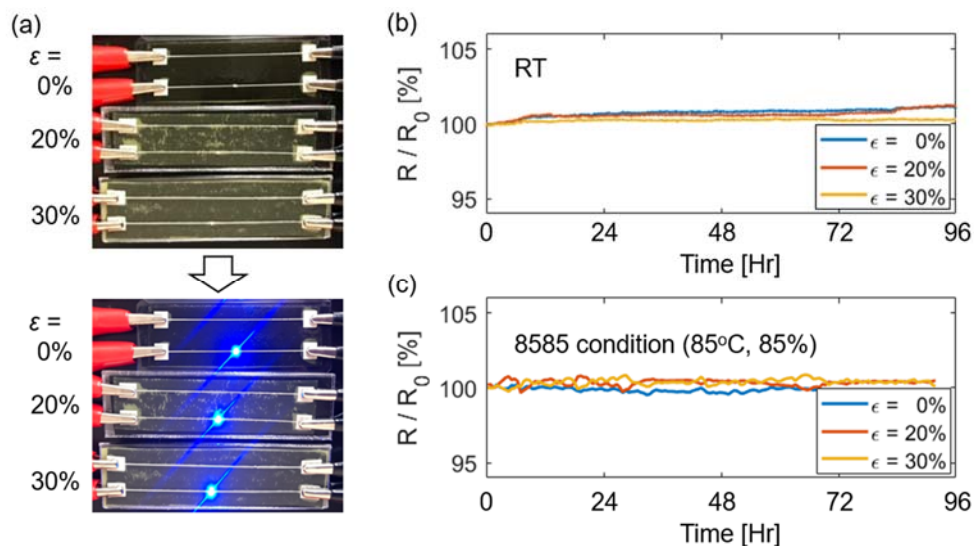


Fig. 3. (a) Photograph of longitudinally stretched Ag flake-based electrode/substrate before and after operation of the photodiode, (b) trend of resistance change over time measured at room temperature and (c) trend of resistance change over time, measured in an 85/85 condition (i.e., 85°C and 85% relative humidity).

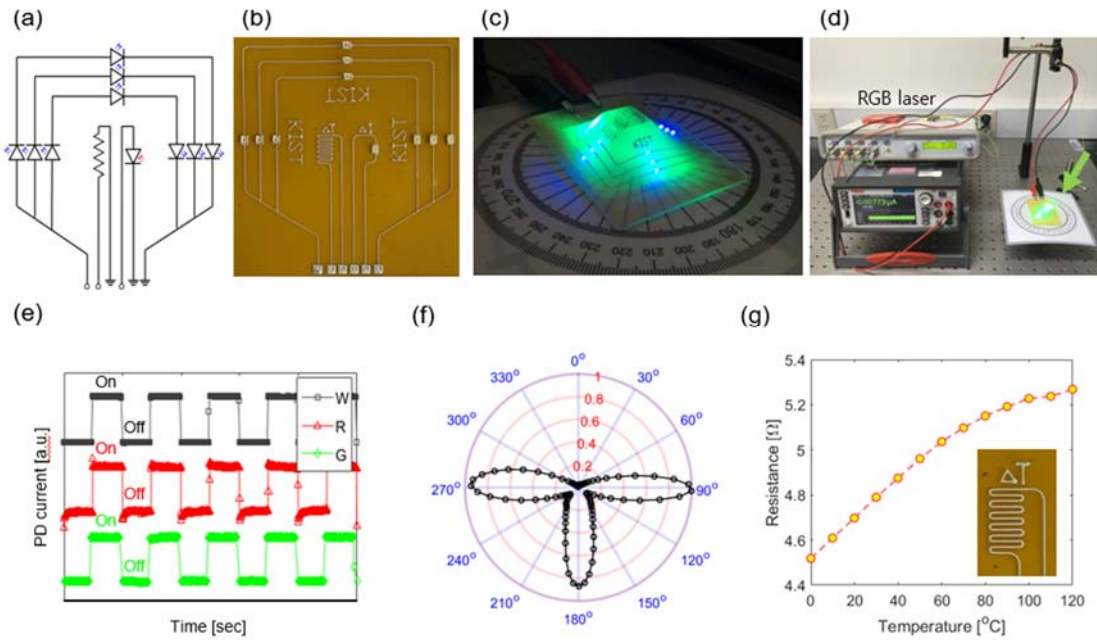


Fig. 4. (a) Circuit diagram of multi-functional FPCB device, (b) conductive ink pattern drawn on flexible/stretchable substrate, (c) completed 3D FPCB in operation, (d) configuration of angular photo-sensing sensor, (e) calibration of photo-sensors on 3D FPCB, (f) photo-current at different optical excitation azimuthal angle (black circles: normalized photo-current), and (g) calibration of temperature sensor on 3D FPCB.

facilitating connectivity between these components. Figures 4(b) and (c) show photographs of the sensor element in its initial flat state and after three-dimensional thermal deformation, respectively, constructed according to the aforementioned circuit schematic. Notably, Fig. 4(c) demonstrates that the photodiodes within the prototype of the three-dimensional sensor element are positioned to capture light from multiple directions, showcasing uniform light emission characteristics. This method marks a significant advancement over traditional fabrication processes, enabling the creation of stable, omnidirectionally oriented devices through a simplified procedure. Figure 4(d) illustrates the infrastructure designed for analyzing environmental response characteristics exhibited by the three-dimensional sensor elements. When exposed to external light, the photodiode within the sensor generates a photocurrent, while the RTD's resistance value changes in response to temperature variations. This infrastructure integrates components for irradiating the sensor with RGB lasers and a measurement instrument to monitor the resulting current from the three-dimensional sensor. The photocurrent response characteristics of the three-dimensional sensor to irradiation with red (473 nm), green (532 nm), and white light are summarized in Fig. 4(e). The

graph clearly depicts the fluctuation of the photodiode current (PD current) in response to the activation (on) and deactivation (off) of the three light sources. Additionally, the polar coordinate graph presented in Fig. 4(f) illustrates the ability of the three-dimensionally oriented photodiode array to accurately measure the azimuthal direction of an external light source. Figure 4(g) provides a detailed analysis of the variation in resistance relative to the ambient temperature surrounding the three-dimensional sensor. By correlating the observed resistance values with temperature readings upon activation of the RTD, it becomes possible to deduce the environmental temperature in which the three-dimensional sensor is located.

4. CONCLUSION

The research presented here successfully demonstrates the feasibility of fabricating FPCBs capable of being deformed into three-dimensional shapes while retaining their functional integrity. This achievement marks a significant departure from conventional FPCB designs, which are limited by their flexibility and formability. Through meticulous optimization of the thermal deformation process and the use of Ag flake-

based conductive ink on a modified polyimide substrate, we have established a foundational approach that significantly enhances the adaptability of FPCBs to complex shapes. The practical application of this technology was evidenced in the creation of a prototype sensor device, showcasing its ability to function reliably in a three-dimensional form. This device, with its integrated photodiode and temperature sensor, demonstrates not only the robustness of the developed FPCB but also its potential for broad application in future electronic devices. By addressing the challenges of electronic circuit integration into diverse product forms, this study contributes to the advancement of wearable electronics, transformable displays, and other innovative technologies. Future work will focus on refining this technology to support a wider range of electronic components and exploring its integration into commercial products, aiming to meet the growing demand for adaptable and functionally diverse electronic devices.

ORCID

Jae-Min Hong
Seoung-Ki Lee

<https://orcid.org/0000-0001-9238-5451>
<https://orcid.org/0000-0002-8786-0251>

ACKNOWLEDGMENTS

This research was supported from the Ministry of Trade, Industry & Energy of Korea (0269589) and the Nano & Material Technology Development Program through the National Research Foundation of Korea (NRF) funded by Ministry of Science and ICT (NRF-2021M3H4A6A03103770).

REFERENCES

- [1] Z. Hui, L. Zhang, G. Ren, G. Sun, H. D. Yu, and W. Huang, *Adv. Mater.*, **35**, 2211202 (2023).
doi: <https://doi.org/10.1002/adma.202211202>
- [2] X. Zhang, Z. Hu, Q. Sun, X. Liang, P. Gu, J. Huang, and G. Zu, *Angew. Chem. Int. Ed.*, **62**, e202213952 (2023).
doi: <https://doi.org/10.1002/anie.202213952>
- [3] M. Khaouani, H. Bencherif, and A. Meddour, *Trans. Electr. Electron. Mater.*, **23**, 113 (2021).
doi: <https://doi.org/10.1007/s42341-021-00328-x>
- [4] K. I. Jang, S. Y. Han, S. Xu, K. E. Mathewson, Y. Zhang, J. W. Jeong, G. T. Kim, R. C. Webb, J. W. Lee, T. J. Dawidczyk, R. H. Kim, Y. M. Song, W. H. Yeo, S. Kim, H. Cheng, S. I. Rhee, J. Chung, B. Kim, H. U. Chung, D. Lee, Y. Yang, M. Cho, J. G. Gaspar, R. Carbonari, M. Fabiani, G. Gratton, Y. Huang, and J. A. Rogers, *Nat. Commun.*, **5**, 4779 (2014).
doi: <https://doi.org/10.1038/ncomms5779>
- [5] M. Kim, K. Y. Ma, H. Kim, Y. Lee, J. H. Park, and H. S. Shin, *Adv. Mater.*, **35**, 2205520 (2023).
doi: <https://doi.org/10.1002/adma.202205520>
- [6] S. H. Kang, J. W. Jo, J. M. Lee, S. Moon, S. B. Shin, S. B. Choi, D. Byeon, J. Kim, M. G. Kim, Y. H. Kim, J. W. Kim, and S. K. Park, *Nat. Commun.*, **15**, 2814 (2024).
doi: <https://doi.org/10.1038/s41467-024-47184-w>
- [7] D. H. Kim, N. Lu, Y. Huang, and J. A. Rogers, *MRS Bull.*, **37**, 226 (2012).
doi: <https://doi.org/10.1557/mrs.2012.36>
- [8] I. S. Yoon, S. H. Kim, Y. Oh, B. K. Ju, and J. M. Hong, *Sci. Rep.*, **10**, 5036 (2020).
doi: <https://doi.org/10.1038/s41598-020-61752-2>
- [9] S. Gandla, S. Kang, J. Kim, Y. Yu, J. Kim, H. Lim, H. J. Kwon, S. M. Park, and S. Kim, *IEEE Internet Things J.*, **11**, 15656 (2024).
doi: <https://doi.org/10.1109/JIOT.2024.3350022>
- [10] G. Sun and H. Zhao, *Trans. Electr. Electron. Mater.*, **24**, 267 (2023).
doi: <https://doi.org/10.1007/s42341-023-00447-7>
- [11] P. Naik, A. Nayak, and S. K. Patri, *Trans. Electr. Electron. Mater.*, **24**, 149 (2023).
doi: <https://doi.org/10.1007/s42341-022-00425-5>
- [12] W. Lee, J. Woo, S. Lee, and H. Lee, *Sens. Actuators, A*, **367**, 115026 (2024).
doi: <https://doi.org/10.1016/j.sna.2024.115026>
- [13] K. Sun, G. Wu, K. Liang, B. Sun, and J. Wang, *Micromachines*, **14**, 1020 (2023).
doi: <https://doi.org/10.3390/mi14051020>
- [14] J. Kim, J. Im, J. Ko, S. Lee, D. Kwon, W. Shin, J. Hwang, R. H. Koo, W. Y. Choi, and J. H. Lee, *Proc. 2023 International Electron Devices Meeting (IEDM)* (IEEE, San Francisco, USA, 2023).
doi: <https://doi.org/10.1109/IEDM45741.2023.10413852>
- [15] Z. W. Lin, S. L. Qi, and D. Z. Wu, *J. Appl. Polym. Sci.*, **125**, 3552 (2012).
doi: <https://doi.org/10.1002/app.36240>
- [16] H. K. Choi, A. Lee, M. Park, D. S. Lee, S. Bae, S. K. Lee, S. H. Lee, T. Lee, and T. W. Kim, *ACS Nano*, **15**, 829 (2021).
doi: <https://doi.org/10.1021/acsnano.0c07352>
- [17] Y. Wang, P. Zhu, W. Li, X. Liu, H. Li, Y. Deng, and M. Tan, *ACS Appl. Mater. Interfaces*, **14**, 12920 (2022).
doi: <https://doi.org/10.1021/acsmi.2c00542>